Turk J Chem
36 (2012) , 111 – 120.

doi:10.3906/kim-1104-61

Hydrothermal synthesis and characterization of nanosized transition metal chromite spinels

Shahid Khan DURRANI[1,*], **Syed Zahid HUSSAIN**[1], **Khalid SAEED**[1], **Yaqoob KHAN**[2], **Mohammad ARIF**[1], **Nisar AHMED**[1]

[1] *Materials Division, Directorate of Technology, Pakistan Institute of Nuclear Science and Technology, Islamabad-PAKISTAN*

e-mail: durranisk@ gmail.com

[2] *Department of Chemical and Materials Engineering, Pakistan Institute of Engineering and Applied Sciences, Islamabad-PAKISTAN*

Received: 26.04.2011

Homogeneous crystalline transition metal chromite spinels (MCr_2O_4, where M = Co, Mn, and Ni) were prepared by hydrothermal reaction of aqueous solutions containing the respective metal nitrate, chromium(III) nitrate, and sodium hydroxide in stoichiometric amounts at 180-200 °C and pH 10.5-11.5 for 11-13 h. The crystalline structure, microstructure, and thermal stability of the synthesized chromite products were analyzed by X-ray diffraction (XRD), scanning electron microscopy, thermogravimetry, and differential thermal analysis. The analysis results revealed that the $CoCr_2O_4$ and $MnCr_2O_4$ crystalline phases were thermally stable in the range of 750-800 °C. UV-visible studies showed that higher characteristic bands corresponded to the region of the visible spectrum of cobalt ($CoCr_2O_4$, bluish-green) and manganese-doped cobalt chromites ($Co_{0.5}Mn_{0.5}Cr_2O_4$, dark green). XRD powder diffraction data of specimens revealed the formation of a well-crystallized spinel structure of transition metal chromite (approximately 98%) after calcination at 550-750 °C. The nanocrystallinity of synthesized $CoCr_2O_4$ was found to be in the range of approximately 100-120 nm.

Key Words: Hydrothermal synthesis, nanocrystalline, chromite, spinel, microstructure, X-ray diffraction, thermogravimetry, differential thermal analysis

Introduction

Chromite ($FeO.Cr_2O_3$) is one of the principal ores of chromium and is found in peridotite, intrusive igneous rocks.[1–3] It is commonly associated with olivine, magnetite, serpentine, and corundum.[4] In Pakistan, chromite

*Corresponding author

is located in the Muslim Bagh area of the Zhob district of Balochistan. Most of the chromite is of metallurgical grade with 40% Cr_2O_3 and a chrome-to-iron ratio of 2.6:1. Spinel is an important class of mixed-metal oxides and has the general chemical composition of AB_2O_4 where A and B are cations occupying tetrahedral and octahedral sites, respectively. Normally, A is a divalent and B is a trivalent atom. The cations occupy only one-eighth of the tetrahedral sites and one-half of the octahedral sites.[5–8] Transition metal chromites MCr_2O_4 (where M = Co, Cu, Mn, Ni, and Zn), with spinel-like structures, have attracted much attention because of their tremendous technological importance as heat resistant pigments,[9] refractories with optical properties,[10] and protective coating materials for interconnects in solid oxide fuel cell stack systems,[11] as well as catalysts for the decomposition of chlorinated organic pollutants.[12] $CoCr_2O_4$, $MnCr_2O_4$, and $NiCr_2O_4$ are ferromagnetic spinels; in single-crystal samples, the collinear ferrimagnetic ordering occurs at T_c = 51 K, 93 K, and 74 K for Mn, Co, and Ni, respectively. Yamasaki et al.[13] reported the presence of ferroelectricity in $CoCr_2O_4$. Zinc chromites ($ZnCr_2O_4$) are effective catalyst materials for the synthesis of biodiesel and the removal of methane from compressed natural gas engines and sensor materials.[14,15] Copper chromite ($CuCr_2O_4$) spinel is one of the most effective catalysts for CO oxidation in automobile-emission control and is also used as a burning catalyst to increase the rates of combustion of solid rocket propellants. It increases the burning rate of propellants at all pressures, producing a good catalytic effect on the decomposition and deflagration rate of ammonium perchlorate and polystyrene solid composite.[16]

The most widely used method for the synthesis of chromite spinels involves solid-state reaction metal oxides at high temperatures.[17,18] Solid-state reaction requires the long-range diffusion of metal ions, which may result in inhomogeneity, larger and nonuniform grains (micron-sized), and poor control of stoichiometry. The unavoidable sintering caused by the high-temperature calcination leads to materials with a small surface area. In recent years, wet chemical routes have been used for the synthesis of homogeneous, sinterable chromite powders with large surface areas. In the wet chemical process, the powders are synthesized in liquid systems by means of coprecipitation,[19] microemulsion,[20] citrate-nitrate gel combustion,[21] sol-gel,[22] sol-spray processes,[23,24] polymeric gel,[25] and hydrothermal processes.[26,27] Among these methods, hydrothermal processes have the major advantage of preparing homogeneous, fine crystalline oxide materials with controlled particle size and morphology. The hydrothermal method is a cost-effective and easy route for preparing fine crystalline oxides at low temperatures and in a short reaction time.[28] The aim of the present work was to develop a low-temperature hydrothermal route to synthesize nanosized transition metal chromite spinels. Microstructure evaluation and examination of the crystallization phase and thermal decomposition behavior of synthesized chromite spinels were conducted with scanning electron microscopy (SEM), X-ray diffraction (XRD), thermogravimetry (TG), and differential thermal analysis (DTA) techniques.

Experimental

Materials

The starting materials used in the present study were cobalt nitrate 6-hydrate ($Co(NO_3)_2.6H_2O$), copper nitrate 3-hydrate ($Cu(NO_3)_2.3H_2O$), manganese nitrate 4-hydrate ($Mn(NO_3)_2.4H_2O$), nickel nitrate 6-hydrate ($Ni(NO_3)_2.6H_2O$), and chromium nitrate 9-hydrate ($Cr(NO_3)_3.9H_2O$) (all from Merck, 99.9%), and sodium hydroxide pellets (NaOH, Merck). All chemicals were of analytical reagent grade and were used without further purification.

Procedure

Transition metal chromites MCr_2O_4 (M = Co, Cu, Mn, and Ni) were synthesized by a hydrothermal process according to the conditions given in Table 1. In a typical synthesis procedure, aqueous solutions containing the respective metal chloride or nitrate and chromium(III) nitrate in different molar proportions were combined and dissolved in a 250-mL evaporator flask. A NaOH aqueous solution (10 M) was added dropwise and the pH of the suspension was maintained at 10.5-11.5 with an attached pH regulator. The evaporator flask was fitted in a rotary apparatus (Laborota 4001, Heidolph) and maintained at a temperature of 70-80 °C for 4 h until a homogeneous suspension was obtained. The suspension was transferred to a polytetrafluoroethylene-lined stainless steel digestion bomb, which was kept in an oven at 180-200 °C for 11-13 h and finally cooled to room temperature in the oven. The resulting white precursor was collected and washed with acid (0.1 N HCl), followed by rinsing in deionized water and absolute ethanol alternately to remove the NaOH until a neutral pH was obtained. The precursor was dried at 90 °C for 6 h in an oven. Finally, a dark green, soft powder was obtained. The dried powder specimens were calcined at different temperatures (500-850 °C) for 4 h.

Table 1. Hydrothermal reaction conditions for formation of transition metal chromites.

Specimens	Molar proportion		Reaction conditions		
	M^{2+}/Cr^{3+}	Na^{+}/Cr^{3+}	pH	Temperature (°C)	Time (h)
$CoCr_2O_4$	0.5	2.5	10.5	180	11
$MnCr_2O_4$	0.6	2.6	10.5	200	12
$Co_{0.5}Mn_{0.5}Cr_2O_4$	0.5	1.5	11.0	200	13
$NiCr_2O_4$	0.6	2.9	10.0	200	13
$CuCr_2O_4$	0.5	2.5	10.3	180	11
$Ni_{0.8}Cu_{0.2}Cr_2O_4$	0.6	2.8	11.5	200	12

Characterization

The thermal stability, dehydration, and decomposition of the synthesized powders were studied by TG and DTA using a simultaneous thermogravimetric analyzer (STA-409, NETZSCH) with a temperature-programmed furnace. All of the specimens were heated in a temperature range from ambient to 1000 °C in air with a heating rate of 10 °C/min. The crystallinity and phase analyses were conducted by XRD using a Geiger flux instrument (Rigaku) with CuK_α radiation ($\lambda = 0.154056$ nm). The XRD data were collected in the 2θ range from $15° < 2\theta < 80°$ with step-scanning increments of 0.05° and a scanning rate of 5°/min. The morphologies of the metal chromites were observed by SEM (JEOL). The sample for SEM observation was prepared by 10 min of ultrasonic dispersion of a small amount of sample in ethanol, and a drop of the solution was put onto a clean and polished aluminum stud and coated with a thin layer of gold. The densities of the powder chromite materials were measured with an Ultrapycnometer 1000 (Quantachrome). UV-visible absorption spectra were measured with a UV-Vis spectrophotometer (Specord 205, Analtik Jena). In order to obtain transparent colored phases, the chromites were dissolved in a phosphoric acid solution process.[29]

Results and discussion

The thermogravimetric thermograms of $CoCr_2O_4$ and $MnCr_2O_4$ chromite powders are shown in Figures 1a and 1b. The weight loss from room temperature to about 750 °C was 32.7% and 26.5% in the cobalt and manganese chromites, respectively. Figures 2a and 2b show the DTA thermograms of $CoCr_2O_4$ and $MnCr_2O_4$ powders, respectively. The DTA endothermic peak$_{max}$ at 102 °C (Figure 2a, $CoCr_2O_4$) and at 127 °C (Figure 2b, $MnCr_2O_4$) can be attributed to the dehydration of adsorbed water molecules. The endothermic peak$_{max}$ values at 321 and 418 °C (Figure 2a, $CoCr_2O_4$) and at 338 and 423 °C (Figure 2b, $MnCr_2O_4$) are due to the decomposition of partial hydroxyl and loosely bound nitrates. The exothermic peak around 524 °C (Figure 2a, $CoCr_2O_4$) is due to the initiation of a crystallization reaction of cobalt chromite ($CoCr_2O_4$) within the cobalt and chromium hydroxide gel. The exothermic peak around 768 °C shows the phase transformation from cobalt and chromium hydroxide to the complete crystallization of cobalt chromite ($CoCr_2O_4$). Similarly, the exothermic peak at 460 °C (Figure 2b, $MnCr_2O_4$) is due to the initiation of a crystallization reaction of manganese chromite ($MnCr_2O_4$) within the manganese and chromium hydroxide gel. The second exothermic peak at 770 °C shows the phase transformation from manganese and chromium hydroxide to the complete crystallization of manganese chromite ($MnCr_2O_4$). At these stages, weight loss was observed for the residue of the alkaline solution. However, no further weight loss and no thermal effects occurred beyond these exothermic peaks, indicating that decomposition does not occur above this temperature and that the stable residues may be ascribed to $CoCr_2O_4$ particles. The TG curves also show that there were no weight changes at the end of the decomposition reaction after 700 °C. These results reveal that the $CoCr_2O_4$ and $MnCr_2O_4$ crystalline phases are thermally stable at 800 °C.[30] An overview of the weight loss percentages and thermal stability of the transition metal chromites is given in Table 2.

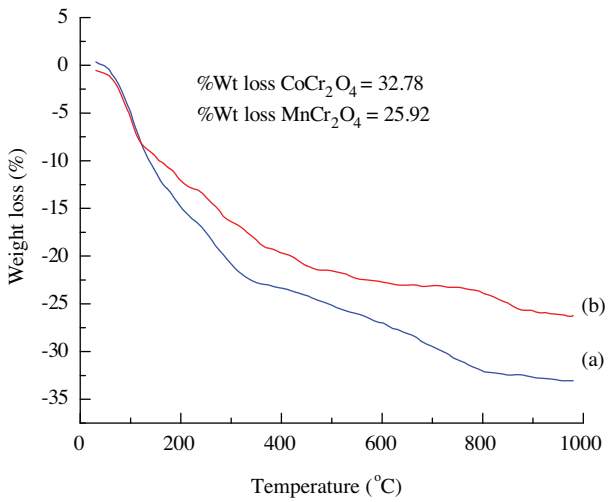

Figure 1. TG curves of transition metal chromite spinels: a) $CoCr_2O_4$ and b) $MnCr_2O_4$.

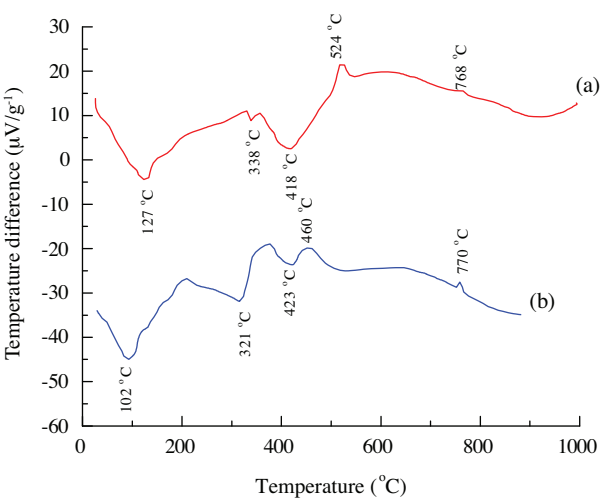

Figure 2. DTA curves of transition metal chromite spinels: a) $CoCr_2O_4$ and b) $MnCr_2O_4$.

Figures 3a and 3b show the UV-Vis absorption spectra of $CoCr_2O_4$ (Figure 3a) and $Co_{0.5}Mn_{0.5}Cr_2O_4$ (Figure 3b) solutions as a function of wavelength, in nanometers. The characteristic bands around 345-365 nm are clearly pronounced in the optical absorption spectra of the chromite spinels. These bands are due to the

assignments of Cr^{3+} ions in the octahedral coordination. Additional bands at around 630-685 nm in the spectra of cobalt chromite can be attributed to cobalt in the octahedral coordination. The appearance of these bands is due to the interaction between cobalt, manganese, and chromium salts to form chromite spinel. These higher bands correspond to the bluish-green/dark green region of the visible spectrum (654-694 nm).[31]

The Fourier transform infrared (FTIR) spectra of $CoCr_2O_4$ and $Co_{0.5}Mn_{0.5}Cr_2O_4$ are shown in Figures 4a and 4b. The infrared (IR) bands of other chromites ($MnCr_2O_4$, $NiCr_2O_4$, $CuCr_2O_4$, and $Ni_{0.5}Cu_{0.5}Cr_2O_4$) are given in Table 2. Transition metal chromite spinels are expected to exhibit the characteristic absorption bands in the shortwave region around 690-650 cm^{-1}, 580-540 cm^{-1}, and 530-485 cm^{-1} due to M-O and Cr-O stretching frequencies, respectively.[32] The IR bands (600-540 cm^{-1}) for all chromite samples could be attributed to the stretching vibration of the Cr-O bands of chromium atoms in the tetragonal environment of the O atom. In the case of $CoCr_2O_4$, the vibration frequency at 665 cm^{-1} is characteristic of Co-O stretching modes in octahedral sites, i.e. the displacement of oxide anions relative to the chromium cations in the direction of octahedral chains. Some properties of the transition metal chromites, such as density, weight loss percentage, thermal stability, visible absorption bands, and IR bands, are summarized in Table 2. The powder densities of MCr_2O_4 are in the range of 70%-85% of the theoretical density.

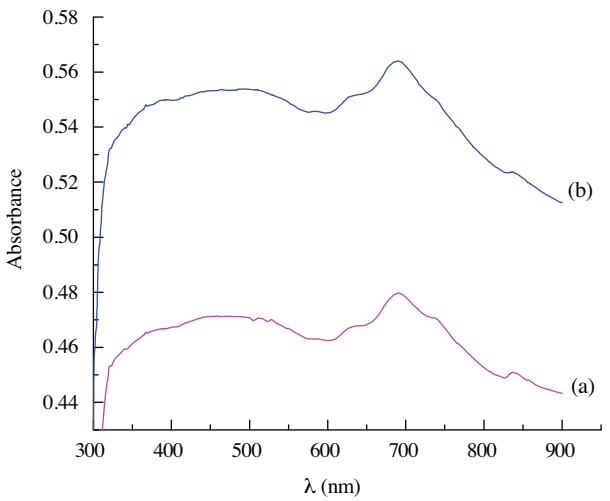

Figure 3. UV-visible spectra of transition metal chromite spinels: a) $CoCr_2O_4$ and b) $Co_{0.5}Mn_{0.5}\ Cr_2O_4$.

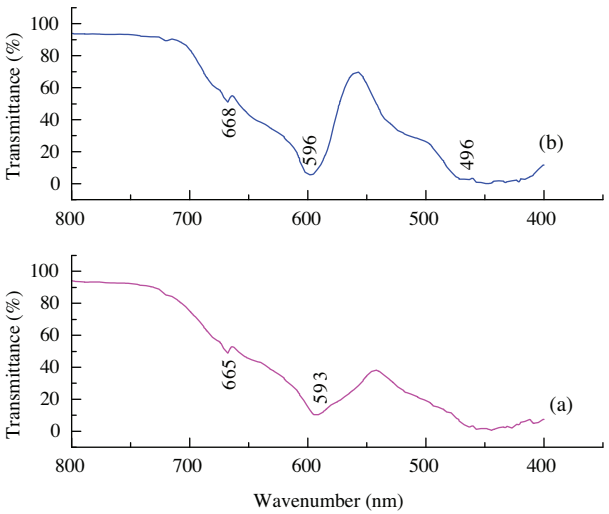

Figure 4. FTIR spectra of transition metal chromite spinels: a) $CoCr_2O_4$ and b) $Co_{0.5}Mn_{0.5}Cr_2O_4$.

Figures 5a-5c show the XRD patterns of dried (100 °C) and calcined (550 and 750 °C) cobalt chromite powders. The sharp and broad peaks appearing in the diffractograms in Figures 5b and 5c confirm the formation of a fine nanocrystalline, single-phase chromite spinel structure. A few characteristic peaks of chromium oxide (Cr_2O_3) were also observed. The main peak (Figure 5c) was centered at $2\theta = 35.85°$ and corresponds to a crystal plane with Miller indices of 311, which is characteristic of the peak of face-centered cubic (FCC) spinel $CoCr_2O_4$.[33] The other sharp peaks in the XRD patterns were compared and were found to be similar to the reported FCC spinel JCPDS 22-1084.[34] The relatively sharp peaks were indexed and analyzed with unit cell refinement.[35] The results revealed that synthesized $CoCr_2O_4$ is a FCC spinel with cell parameter a = 8.315 Å, unit cell volume = 575 $Å^3$, and space group = Fd3m. The grain size, as determined by Scherrer's

formula,[36] of $CoCr_2O_4$ dried at 110 °C and calcined at 550 and 750 °C was approximately 90, 105, and 112 nm, respectively. The XRD results revealed that an increase in calcination temperature leads to a considerable increase in peak intensity. Meanwhile, the widths of the diffraction peaks become narrower with the increase of calcination temperature, indicating that the size of the particles increases.

Table 2. Physicochemical analysis of alkaline earth metal chromites.

Chromite materials	Powder density (g mL^{-1})	Weight loss (%)	Thermal stability (°C)	Visible absorption (λ_{maxima})	FTIR absorption bands (ν^{-}_{maxima})
$CoCr_2O_4$	4.22	32.8	800	685	593, 665
$MnCr_2O_4$	3.85	25.9	750	678	585, 660
$Co_{0.5}Mn_{0.5}Cr_2O_4$	4.16	28.5	850	690	596, 668
$NiCr_2O_4$	3.95	24.6	800	694	535, 645
$CuCr_2O_4$	4.15	22.4	750	654	568, 640
$Ni_{0.8}Cu_{0.2}Cr_2O_4$	3.94	16.5	850	684	579, 660

The XRD patterns and phase analysis of $MnCr_2O_4$, $NiCr_2O_4$, $Co_{0.5}Mn_{0.5}Cr_2O_4$, and $Ni_{0.8}Cu_{0.2}Cr_2O_4$ are presented in Figures 6a-6c, Figures 7a-7c, and Figures 8a and 8b, respectively. The sharp peaks appearing in the diffractograms indicate the presence of an ordered crystalline metal chromite phase with a spinel structure along with a Cr_2O_3 phase (approximately 2.5%). The mean crystallite sizes of these specimens, calculated by Scherrer's formula, are given in Table 3.

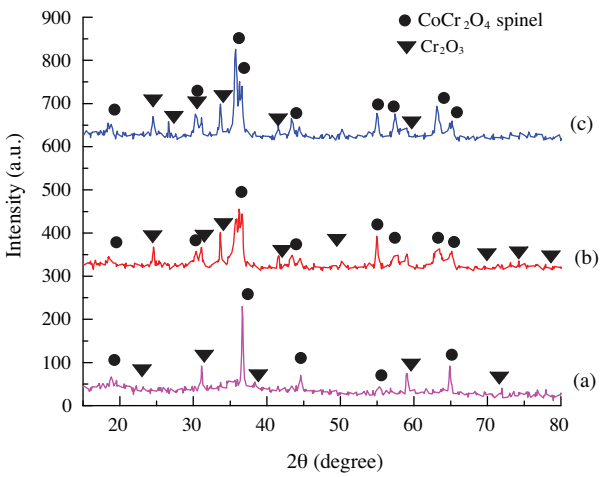

Figure 5. XRD patterns of cobalt chromite spinels, $CoCr_2O_4$: a) dried at 110 °C, b) calcined at 550 °C in air for 4 h, and c) calcined at 750 °C in air for 4 h.

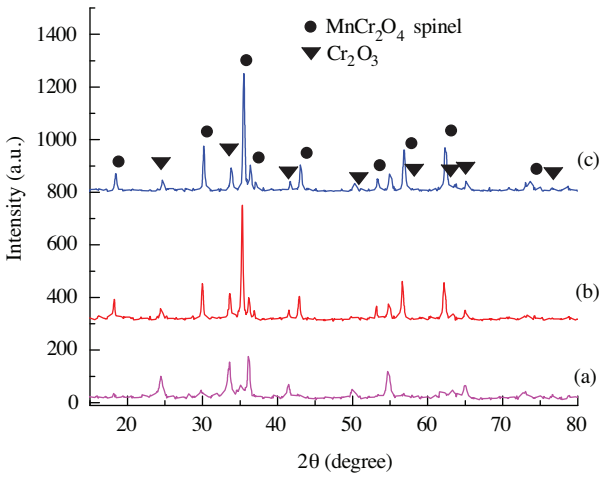

Figure 6. XRD patterns of manganese chromite spinels, $MnCr_2O_4$: a) powder calcined at 550 °C in air for 4 h, b) calcined at 750 °C in air for 4 h, and c) calcined at 850 °C in air for 4 h.

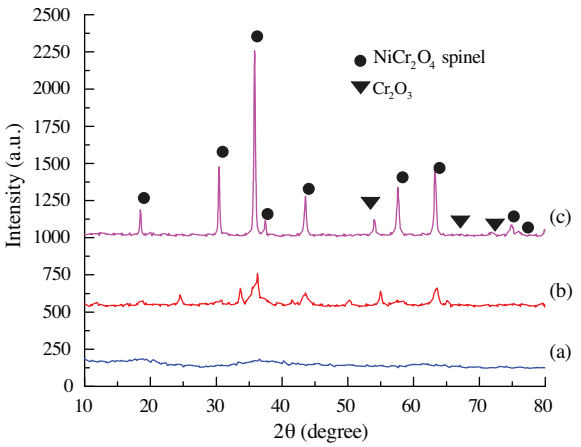

Figure 7. XRD patterns of nickel chromite spinels, $NiCr_2O_4$: a) powder dried at 110 °C, b) calcined at 550 °C in air for 4 h, and c) calcined at 750 °C in air for 4 h.

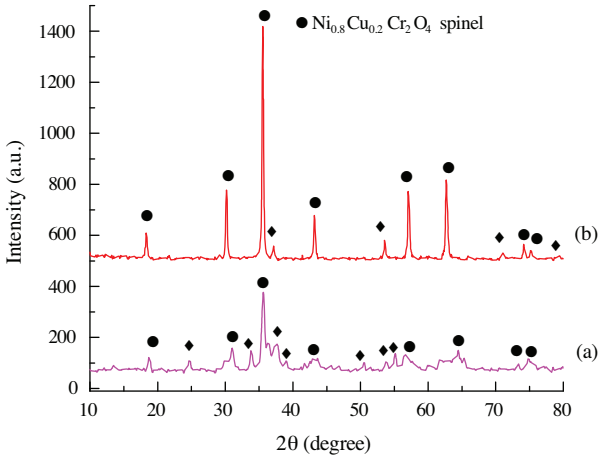

Figure 8. XRD patterns of nickel- and copper-doped chromite spinels: a) $Ni_{0.8}Cu_{0.2}Cr_2O_4$ calcined at 750 °C in air for 4 h and b) $Co_{0.5}Mn_{0.5}Cr_2O_4$ calcined at 850 °C in air for 4 h.

Table 3. XRD analysis of hydrothermally synthesized transition metal chromites.

Metal chromites	XRD phase		Mean crystallite size (nm)	Cell parameter (%)		Cell volume $(Å)^3$	Symmetry	JCPDS card no.[34]
	Cr_2O_3	MCr_2O_4						
$CoCr_2O_4$	2.6	97.4	112 ± 1.4	8.315		575	Cubic	22-084
$MnCr_2O_4$	2.5	97.5	125 ± 2.5	8.428		598	Cubic	75-1614
$Co_{0.5}Mn_{0.5}Cr_2O_4$	1.8	98.2	128 ± 5.5	8.328		578	Cubic	70-2645
$NiCr_2O_4$	2.2	97.8	123 ± 4.7	8.297		571	Cubic	75-1728
$CuCr_2O_4$	1.8	98.2	135 ± 8.7	6.029	7.768	282	Tetragonal	34-0424
$Ni_{0.8}Cu_{0.2}Cr_2O_4$	3.6	96.4	121 ± 5.9	5.987	7.737	277	Tetragonal	37-0224

M = Co, Mn, and Ni

Figures 9a-9c show the morphologies of $CoCr_2O_4$ powder dried at 110 °C, as measured by SEM at different magnifications. It can be observed that the $CoCr_2O_4$ powder primarily consists of aggregated microcrystals with an average grain size of about 1 μm (Figure 9a). Uniform nanosized crystals of $CoCr_2O_4$ can be seen at higher magnifications in Figures 9b and 9c. The mean diameter of the nanocrystals is <100 nm, which is in approximate agreement with the grain size (approximately 90 nm) as measured by Scherrer's formula using XRD data.

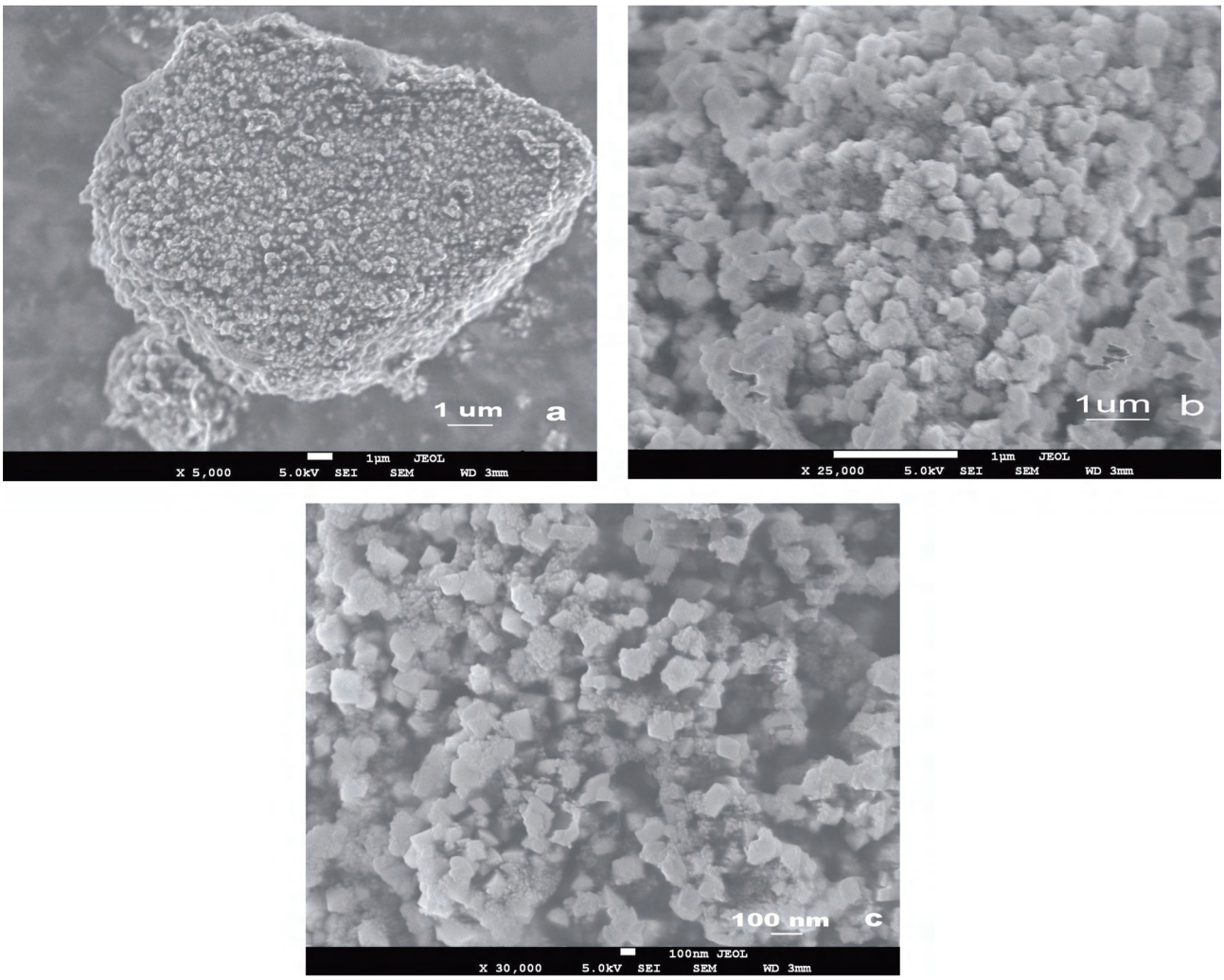

Figure 9. SEM images of cobalt chromite spinel nanocrystals, $CoCr_2O_4$, obtained at 110 °C with different magnifications: a) at × 5000, b) at × 25,000, and c) at × 30,000.

Conclusions

Nanocrystalline transition metal chromite spinels such as $CoCr_2O_4$ (bluish-green), $MnCr_2O_4$ (grayish-green), $Cu_{0.5}Mn_{0.5}Cr_2O_4$ (green), $NiCr_2O_4$ (sage green), $CuCr_2O_4$ (blackish-green), and $Ni_{0.8}Cu_{0.2}Cr_2O_4$ (dark green) were synthesized successfully through a hydrothermal method. The formation of the spinel phase, crystalline chromites, was confirmed by characteristic powder XRD. The physicochemical and thermal analysis showed that the synthesized metal chromite products have a high percentage of the desired chromite spinel phase and are thermally stable at up to 800 °C. The results revealed that the average particle size was in the range of approximately 100-120 nm. The XRD studies showed that MCr_2O_4 (M = Co, Cu, Mn, and Ni) has a FCC spinel structure.

Acknowledgements

The authors wish to thank N. Khalid and Azhar Mashiatullah for their technical assistance during FTIR and UV-Vis specimen preparation.

References

1. Rubie, D. C.; Duffy, T. S.; Ohtani, E. *New Developments in High-Pressure Mineral Physics and Applications*, Elsevier, San Diego, CA, 2004.
2. Boehler, R. *Rev. Geophys.* **2000**, *38*, 221-245.
3. Pownceby, M.; Bourne, P. *Mineral. Mag.* **2006**, *70*, 51-64.
4. Aye, S. W. H.; Lwin, K. T.; Oo, W. W. K. K. *World Academy Sci. Engineer. Tech.* **2008**, *46*, 569-571.
5. Marinkovi Stanojevi, Z. V.; Romevi, N.; Stojanovi, B. *J. Eur. Ceram. Soc.* **2007**, *27*, 903-907.
6. Julien, C. M.; Gendron, F.; Amdouni, A.; Massot, M. *Mater. Sci. Eng. B* **2006**, *130*, 41-48.
7. Wulfsberg, G. *Inorganic Chemistry*, University Science Books, Sausalito, CA, 2000.
8. Zayat, M.; Levy, D. *Chem. Mater.* **2000**, *12*, 2763-2769.
9. Ahmed, I. S.; Dessouki, H. A.; Ali, A. A. *Polyhedron* **2011**, *30*, 584-591.
10. Khalil, N. M.; Hassan, M. B.; Ewais, E. M. M.; Saleh, F. A. *J. Alloy. Comp.* **2010**, *496*, 600-607.
11. Pillis, M. F.; Ramanathan, L. V. *Surf. Engineer.* **2006**, *22*, 129-137.
12. Kim, D. C.; Ihm, S. K. *Environ. Sci. Technol.* **2001**, *35*, 222-226.
13. Yamasaki, Y.; Miyaska, S.; Kaneko, Y.; He, J. P.; Arima, T.; Tokura, Y. *Phys. Rev. Lett.* **2006**, *96*, 207201-207204.
14. Marinkovic Z. V.; Mancic L.; Maric R.; Milosevic O. *J. Euro. Ceram. Soc* **2001**, *21*, 2051-2055.
15. Regina Mary, L.; Jeyaraj, B.; Nagaraja, K. S. *IEEE Sensors & Transducers* **2009**, *108*, 8-14.
16. Kawamoto, A. M.; Pardini, L. C.; Rezende, L. C. *Aerosp. Sci. Technol.* **2004**, *8*, 591-598.
17. Fernández Colinas, J. M.; Otero Areán, C. *J. Solid State Chem.* **1994**, *109*, 43-46.
18. Durrani, S. K.; Akhtar, J.; Hussain, M. A.; Arif, M.; Ahmad, M. *Mat. Chem. Phys.* **2006**, *100*, 324-328.
19. Patil, K. C.; Hegde, M. S.; Rattan, T.; Aruna, S. T. (Eds.) *Chemistry of Nanocrystalline Oxide Materials: Combustion Synthesis, Properties and Applications*, World Scientific Publishing Company, Singapore, 2008.
20. Uskokovi, V.; Drofenik, M. *Surf. Rev. Lett.* **2005**, *12*, 239-277.
21. Durrani, S. K.; Hussain, N.; Saeed, K.; Ahmad, M.; Siddique, M.; Ahmad, N.; Qazi, N. K. *The Nucleus* **2010**, *47*, 17-23.
22. Yazdanbakhas, M.; Khosravi, I.; Goharshadi, E. K.; Youssefi, A. *J. Hazard. Mater.* **2010**, *184*, 684-689.
23. Durrani, S. K.; Qureshi, A. H.; Qayyum, S.; Arif, M. *J. Therm. Anal. Calorim.* **2009**, *95*, 87-91.
24. Durrani, S. K.; Saeed, K.; Qureshi, A. H.; Ahmad, M.; Arif, M.; Hussain, N.; Mohammad, T. *J. Therm. Analy. Calorim.* **2011**, *104*, 645-651.
25. Gama, L.; Ribeiro, M. A.; Barros, B. S.; Kiminami, R. H. A.; Weber, I. T.; Costa, A. C. F. M. *J. Alloy. Comp.* **2009**, *483*, 453-455.

26. Zawadzki, M. *Solid State Sci.* **2006**, *8*, 14-18.
27. Durrani, S. K.; Khan, Y.; Ahmed, N.; Ahmad, M.; Hussain, M. A. *J. Iran. Chem. Soc.* **2011**, *8*, 562-569.
28. Wojciech L. S.; Richard E. R. *Adv. Sci. Tech* **2006** *45* 184-193
29. Anderson, R.; Chapman, N. B. (Eds.) *Sample Pretreatment and Separation*, John Wiley & Sons, Chichester, UK, 1987.
30. Cui, H.; Zayat, M.; Levy, D. *J. Sol-Gel Sci. Tech.* **2005**, *35*, 175-181.
31. Pirogova, G. N.; Panich, N. M.; Korosteleva, R. I.; Voronin, Y. V.; Popova, N. N. *Russian Chem. Bull.* **2001**, *50*, 2377-2380.
32. Pirogova, G. N.; Panich, N. M.; Korosteleva, R. I.; Voronin, Y. V. *Russian Chem. Bull.* **1994**, *43*, 1634-1636.
33. Burdett, J. K.; Price, G. L.; Price, S. L. *J. Am. Chem. Soc.* **1982**, *104*, 92-95.
34. McClune, W. F. (Ed.) *Powder Diffraction File, Inorganic Phases*, International Centre for Diffraction Data, Swarthmore, PA, 1989.
35. Visser, J. W. *J. Appl. Crystallogr.* **1969**, *2*, 89-95.
36. Culity, B. D.; Stock, S. R. *Elements of X-Ray Diffraction*, 2nd ed., Addison-Wesley, Reading, MA, 1978.